



On the Plane Steady Flow of an Ablating Pellet under the Impact of Plasma Electrons

Tang, F.L.; Chang, C.T.

Publication date:
1989

Document Version
Publisher's PDF, also known as Version of record

[Link back to DTU Orbit](#)

Citation (APA):
Tang, F. L., & Chang, C. T. (1989). *On the Plane Steady Flow of an Ablating Pellet under the Impact of Plasma Electrons*. Risø-M No. 2775

General rights

Copyright and moral rights for the publications made accessible in the public portal are retained by the authors and/or other copyright owners and it is a condition of accessing publications that users recognise and abide by the legal requirements associated with these rights.

- Users may download and print one copy of any publication from the public portal for the purpose of private study or research.
- You may not further distribute the material or use it for any profit-making activity or commercial gain
- You may freely distribute the URL identifying the publication in the public portal

If you believe that this document breaches copyright please contact us providing details, and we will remove access to the work immediately and investigate your claim.

3720 348

On the Plane Steady Flow of an Ablating Pellet Under the Impact of Plasma Electrons

F.L. Tang* and C.T. Chang

Risø National Laboratory - Association Euratom

***Permanent address: Institute of Mechanics, Academia Sinica,
Beijing, People's Republic of China**

Sachtitel und Standort:
Zeitschrift, Vol/Nr.:
Reportnummer:

Riso - M - 2775

Page

Overall Record (Gesamtaufnahme) (obligatorisch bei: Rez. Expl.; Büchern/Proceed.; Leading Abstracts)

Data Base* (000):	Subject Categories (008):		
PB <input checked="" type="checkbox"/>	SWO		
ENERGIE (DEL) <input type="checkbox"/>			
INIS DE <input type="checkbox"/> NL <input type="checkbox"/> DK <input checked="" type="checkbox"/> SE <input type="checkbox"/> XC <input type="checkbox"/> CH <input type="checkbox"/>	A 1413	A 1411	
EDB DE <input type="checkbox"/> AT <input type="checkbox"/> CH <input type="checkbox"/> DD <input type="checkbox"/> XE <input type="checkbox"/>			
COAL <input type="checkbox"/> BIOMASS <input type="checkbox"/>			
MATHDI <input type="checkbox"/>	DK (310)		
NTIS <input type="checkbox"/>			
SIGLE <input type="checkbox"/>			
P DATA <input type="checkbox"/> E DATA <input type="checkbox"/>			

Literary Indicator LI (008): W Q N Y E V
Standards Legis. Num. Data Progr. Rep. Abstract (Short Comm.) Comp. Prog. Doc.

Treatment Code TC (008): I Info. C Computing P popular T theor. E exp. M method. D data A appar.

Title in English (200):

Title in German (240):

Title in French (240):

Title Augmentation in Engl. (620):

Title Augmentation in German (623):

Title Augmentation in French (623):

	Page	Input Sheet	Translation required into
Abstract in English:	<input type="text" value="1"/>	<input type="text"/>	en <input type="text"/>
Abstract in German:	<input type="text"/>	<input type="text"/>	de <input type="text"/>
Abstract in French:	<input type="text"/>		

Indexer Date:

Abstractor Date:

Translator Date:

Assignment of Numbers Date:

Descriptive Cataloguer Date:

* Notes:

COAL a/o BIOMASS only together with EDB
INIS-DE only together with EDB-DE
Only non-nuclear energy in EDB AT/CH/DD/XE
SIGLE only for grey Literature from DE
DEL not together with EDB

DE = Federal Republic of Germany
AT = Austria
CH = Switzerland
DD = German Democratic Republic
XE = Commission of the European Communities (CEC)
XC = European Organization for Nuclear Research (CERN)
NL = The Netherlands
DK = Denmark

Links	Descriptors (800)	Data Base	M/Q/D
1	pellet injection		μ_2
2			
3	flu fuel pellets		μ_1
4			
5	plasma flow	P	q2 (P)
6			
7	ablation		q1
8			
9	electron collisions		
10			
11	plasma expansion		q2 (1)
12			
13	" simulation		
14			
15	numerical solution		
16			
17	particle flux	P	
18			
19	scaling laws		
20			
21			
22			
23			
24			
25			
26			
27			
28			
29			

Data Compilation	EDB	D	<input type="checkbox"/>
Compiled Data	INIS	D	<input type="checkbox"/>
Evaluated Data		D	<input type="checkbox"/>
Experimental Data		D	<input type="checkbox"/>
Statistical Data		D	<input type="checkbox"/>
Theoretical Data		D	<input type="checkbox"/>

**On the Plane Steady Flow of an Ablating Pellet Under
the Impact of Plasma Electrons**

F.L. Tang* and C. T. Chang

Risø National Laboratory - Association Euratom

Abstract

To exclude the influence of expansion geometry on the pellet ablation rate, the ideal case of the ablation of a pellet in a constant area duct is considered. As a result of the lack of balance between the heating and the expansion process of the ablatant, a continuous flow is subsonic everywhere. The temperature of the ablatant has a limiting value. The mass ablation flux is determined by the downstream state of the ambient plasma electrons, and influenced by the state of the ablatant at the pellet surface. Compared with either the spherical or cylindrical ablated flow, the pellet ablation rate is more sensitive to the ambient plasma state, and is inversely proportional to the ablatant pressure at the pellet surface

* Permanent address: Institute of Mechanics, Academia Sinica, Beijing, People's Republic of China.

March 1989

Risø National Laboratory, DK-4000 Roskilde, Denmark

ISBN 87-550-1508-5

ISSN 0418-6435

Grafisk Service Risø 1989

CONTENTS

	Page
1. Introduction	5
2. The analytic model	6
2.1. Basic assumptions and governing equations	6
2.2. Normalization	9
2.3. Boundary and compatibility conditions	11
2.4. Approximate solution and scaling law of the mass ablation flux	12
3. Numerical analysis and results	14
4. Discussions	17
4.1. Effect of the magnetic field orientation	17
4.2. Effect of expansion geometry on the pellet ablation rate	17
Acknowledgement	20
References	20
Figurs	21

1. Introduction

As most pellets used in present experiments are cylinders rather than spheres, a study of the influence of the expansion geometry of the ablated flow on the pellet ablation rate has been undertaken. To alleviate the complexity of what is essentially a two-dimensional ablated flow problem of a cylindrical pellet, we have approximated it by a one-dimensional model. This approximation treats the problem in two parts; a cylindrical flow along the radial direction, [1], and a plane flow along the axial direction, [2]. As a result of the constant area approximation for the flow along the ends of the cylinder, a continuous flow is possible only when it is subsonic everywhere. The loss of the transonic feature of the ablated flow clearly indicates that such a crude approximation does not give an adequate description of the flow near the ends of a cylinder.

On the other hand, the plane flow approximation represents an extreme case of ablated flow geometry. By considering a constant area flow of the ablatant, the effect of the geometry on the expansion process is avoided and the ablation process itself might be understood better. The simple geometry also offers the possibility of studying the interaction between the stopping of charged particles and the heating of a gaseous medium. Thus, the study of the plane ablated flow should be of interest in its own right.

The main characteristic of a plane ablated flow, as mentioned above is that a continuous flow is subsonic everywhere. This is a consequence of the absence of the expansion process. A second feature of this lack of expansion is that the ablatant temperature has a limiting value, a thermal choke effect. The subsonic nature of the flow also strongly influences the pellet ablation rate. The ablation rate of the pellet is determined not only by the downstream state of the plasma electrons, but

also by the upstream state of the ablatant at the pellet surface. The mass ablation flux is more sensitive to the ambient state of plasma electrons, than is the spherical or cylindrical ablated flow.

This report is organized into four sections. The analytical model is described in section 2, where the basic assumptions and governing equations are presented first. This is followed by an approximate analytical solution and the scaling law of the mass ablation flux. In section 3, numerical analysis and computational results are given. Finally, in section 4, the effect of magnetic field orientation and that of expansion geometry on the pellet ablation rate are discussed.

2. The analytical model

2.1. Basic assumptions and governing equations

In order to exclude the effect of expansion geometry on the pellet ablation rate itself, we consider the ablation of a pellet in a constant area duct (see Fig. 1). We imagine a cylindrical pellet of solid hydrogen to be inserted at the closed end of a frictionless tube and subjected to the impact of a stream of plasma electrons coming from the open end. A stationary state is assumed to be already established after a brief period of initial bombardment. The pellet thus is shielded by a dense layer of molecular hydrogen gas which acts as a stopping medium for the incoming plasma electrons. The incident plasma electrons are assumed to have a Maxwellian velocity distribution at temperature T_{e0} and particle number density n_{e0} . In view of the lack of information regarding the stopping property of plasma electrons in a medium of variable density, we shall approximate the stream of plasma electrons by an equivalent monoenergetic beam by taking its energy

$$E = 2 T_{eo},$$

and its particle flux,

$$\Phi = \frac{n_{eo}}{4} \left(\frac{8T_{eo}}{nm_e} \right)^{\frac{1}{2}}$$

As an estimate of the maximum ablation rate, we shall take the magnetic field to be normal to the pellet surface. The other extreme case of parallel field orientation will be discussed briefly later.

Taking the ablatant to be a molecular hydrogen gas and a nondissipative medium, the governing equations for the ablated flow can be written as follows.

$$p = \rho T/m \tag{1}$$

$$\frac{d}{dx}(\rho u) = 0 \tag{2}$$

$$\rho u \frac{du}{dx} + \frac{dp}{dx} = 0 \tag{3}$$

$$\rho u \frac{d}{dx} \left(\frac{\gamma}{\gamma-1} \frac{T}{m} + \frac{u^2}{2} \right) = Q(x) \tag{4}$$

where u , p , ρ , T are the velocity, pressure, density, and temperature of the ablatant, respectively. The temperature is given in energy units. $Q(x)$ is the volumetric heat source, i.e. the energy delivered to the ablatant per unit volume per second. To complete the description, we assume $Q(x)$ to be that part of the incoming plasma electron energy flux loss causing the heating and expansion of the ablatant only. Thus

$$Q = f \frac{dq}{dx} \tag{5}$$

Following the argument of ref.[3], we may take $f \approx 0.6$, and

$$\frac{dq}{dx} = \frac{\rho}{m} \Lambda(E)q \quad (6)$$

The attenuation of the energy E is given in turn by the stopping power formula,

$$\frac{dE}{dx} = 2 \frac{\rho}{m} L(E) \quad (7)$$

where $L(E)$ is the loss function. The factor 2 comes from the average of the pitch angles of the incident electrons with respect to the magnetic field lines, [3], and

$$\Lambda(E) = 2 \frac{L(E)}{E} + \sigma(E) \quad (8)$$

thus $\Lambda(E)$ is the energy flux attenuation cross section, and $\sigma(E)$ the total elastic scattering cross section. (Explicit expressions of $L(E)$ and $\sigma(E)$ are given in reference [4].)

Through some algebraic manipulations, it can be shown that the velocity and temperature of the ablatant are given explicitly by

$$\frac{du}{dx} = (\gamma - 1) \frac{mQ}{\rho(\gamma T - mu^2)} \quad (9)$$

$$\frac{dT}{dx} = (\gamma - 1) \frac{mQ}{\rho u} \frac{(T - mu^2)}{(\gamma T - mu^2)} \quad (10)$$

When we anticipate $du/dx > 0$ monotonically, Eq.(9) indicates that the flow field is subsonic everywhere. Eq.(10) further shows that continuous heating of the

ablatant is limited to the range where the local Mach number of the flow, $M^2 < 1/\gamma$. The ablatant temperature reaches a maximum when $M^2 = 1/\gamma$. It is to be noted that this "thermal choke" behaviour is a simple consequence of the presence of a finite heat source and depends neither on the detailed spatial distribution of the source, nor on the detail of its interaction with the ablated flow.

As the entire flow field is subsonic, the solution of the problem, hence the ablation rate of the pellet, is governed both by the downstream state of the unperturbed plasma electrons and by the upstream condition of the ablatant state at the pellet surface. The density ρ_v of the ablatant at the pellet surface depends on the ablation process that takes place at the pellet surface. When the ablation is a sublimation process, one would expect that ρ_v does not exceed ρ_s , the density of solid hydrogen. On the other hand, if the ablation were caused by a dynamic phase transition, [5], $\rho_v > \rho_s$ is possible.

As the velocity, u_v of the ablatant leaving the pellet surface is rather uncertain, then, by using the mass conservation law, Eq.(2), we can replace Eq.(9) by a corresponding equation describing the variation of the ablatant density. Thus,

$$\frac{d\rho}{dx} = - \frac{(\gamma - 1) mQ}{u(\gamma T - mu^2)} \quad (11)$$

2.2 Normalization

Following the previous argument, we shall normalize all variables describing the ablatant state by their corresponding values at the pellet surface, and the state of the slowed-down plasma electrons by its ambient unperturbed values, E_0 and q_0 . The dimensionless variables, denoted by " , " are then

$$\rho' = \rho/\rho_s, \quad T' = T/T_s, \quad u' = u/a_s, \quad q' = q/q_0,$$

$$E' = E/E_0, \quad L' = L(E)/L_0(E_0), \quad \Lambda' = \Lambda(E)/\Lambda(E_0), \quad (12)$$

$$x' = x/A\Lambda_0^{1/2}.$$

where the subscript "s" denotes the corresponding values of the solid hydrogen. Thus $a_s = (\gamma T_s / m)^{1/2}$ is the sound speed corresponding to a surface temperature T_s . Due to the lack of a length scale, we have introduced a characteristic length of $A \Lambda_0^{1/2}$, where A is a numerical factor ($A = 10^5$ is used in the computations).

Considering the normalized mass ablation flux

$$g' = g/\rho_s a_s \quad (13)$$

($\rho_s a_s \approx 2 \text{ kg/cm}^2/\text{s}$ at $T_s = 10 \text{ K}$)

as an eigenvalue of the problem, the ablated flow now is completely described by the following system of equations:

$$\frac{d\rho'}{dx'} = \frac{A_1}{g'} \frac{\Lambda' q' \rho'^2}{\left[\left(\frac{g'}{\rho'} \right)^2 - T' \right]} \quad (14)$$

$$\frac{dT'}{dx'} = \frac{A_1}{g'} \frac{\gamma \left(\frac{g'}{\rho'} \right)^2 - T'}{\left[\left(\frac{g'}{\rho'} \right)^2 - T' \right]} \Lambda' q' \rho' \quad (15)$$

$$\frac{dE'}{dx'} = A_2 \rho' L' \quad (16)$$

$$\frac{dq'}{dx'} = A_3 \rho' q' \Lambda' \quad (17)$$

where

$$A_1 = (\gamma - 1) \frac{iq_0 A \Lambda_0^{3/2}}{m a_s^3} \quad (18)$$

$$A_2 = 2 \left(\frac{\rho_s}{m} \right) \frac{L_0 \Lambda_0^{1/2} A}{E_0} \quad (19)$$

$$A_3 = \left(\frac{\rho_s}{m} \right) \Lambda_0^{3/2} A \quad (20)$$

2.3 Boundary and compatibility conditions

When the surface conditions T_v and ρ_v of the pellet are known and the ambient unperturbed state of the plasma electrons E_0 and q_0 (or T_{e0} and n_{e0}) are given, integration of the system of equations Eqs.(14)- (17) can be initiated at the pellet surface once a proper value of the mass ablation flux g' is chosen and the four variables $\hat{\rho}' = \rho_v / \rho_s$, $\hat{T}' = T_v / T_s$, $\hat{E}' = E_v / E_0$ and $\hat{q}' = q_v / q_0$ are specified at the pellet surface (subscript "v" denotes parameters at the pellet surface). When the ablation of the pellet is caused by the sublimation process, we would expect that

$$\hat{\rho}' \leq 1 \text{ and } \hat{T}' \leq 1 \quad (21)$$

When we expect the existence of a dense layer of ablated gas acting as an effective shield for the incoming electrons, we would expect at the pellet surface that

$$\hat{E}' \rightarrow 0 \text{ and } \hat{q}' \rightarrow 0 \quad (22)$$

The integration is to be terminated at the ablated cloud location

$x' = X'$ where

$$\tilde{E}' (= E/E_0) \rightarrow 1 \text{ and } \tilde{q}' (= q/q_0) \rightarrow 1 \quad (23)$$

In addition, we require that at $x' = X'$

$$\left(\frac{dq'}{dx'} \right)_{x' = X'} \rightarrow 0. \quad (24)$$

Since at $x' = X'$, $\tilde{q}' = \tilde{\Lambda}' = 1$, Eq. (24) is equivalent to the condition that

$$\rho' A_3(E_0) \rightarrow 0, \quad (25)$$

where $\tilde{\rho}' = \rho_f/\rho_s$, and ρ_f is the ablatant mass density at the cloud boundary. Eq.(25) can be viewed, in fact, as a constraint for the proper choice of the normalized mass ablation flux, g' .

2.4. Approximate solution and scaling law of the mass ablation flux

The three conservation laws of mass, momentum, and energy in their dimensionless form can be written as follows:

$$\frac{d}{dx'} (\rho' u') = 0 \quad (26)$$

$$\frac{d}{dx'} (\gamma \rho' u'^2 + \rho' T') = 0 \quad (27)$$

$$\rho' u' \frac{d}{dx'} \left(T' + \frac{\gamma - 1}{2} u'^2 \right) = (\gamma - 1) Q_A \frac{dq'}{dx'} \quad (28)$$

where

$$Q_A = q_0/\rho_s a_s^3 \quad (29)$$

The mass conservation equation can be integrated directly to give the mass ablation flux, g' . Integrating Eq.(27) between the pellet surface, $x'=0$ and the cloud boundary, $x'=X'$, we obtain

$$\tilde{\rho}'\tilde{T}'(1 + \gamma\tilde{M}'^2) = \hat{\rho}'\hat{T}'(1 + \gamma\hat{M}'^2) = \hat{\rho}'\hat{T}' \quad (\because \hat{u} \approx 0) \quad (27a)$$

Integrating Eq.(28) between $x'=0$ and $x'=X'$ and taking into consideration that the total enthalpy at the pellet surface is much less than that at the cloud boundary, we obtain

$$g'\tilde{T}'\left(1 + \frac{\gamma-1}{2}\tilde{M}'^2\right) = (\gamma-1)Q_A(1 - \hat{q}')$$

When we expect the existence of an effective shield mechanism at the pellet surface $\hat{q}' \approx 0$ the above equation reduces to

$$g'\tilde{T}'\left(1 + \frac{\gamma-1}{2}\tilde{M}'^2\right) = (\gamma-1)Q_A \quad (28a)$$

Eliminating T' between Eqs.(27a) and (28a), we obtain

$$\frac{g'}{\tilde{\rho}'} \left(\frac{1 + \frac{\gamma-1}{2}\tilde{M}'^2}{1 + \gamma\tilde{M}'^2} \right) = \frac{(\gamma-1)Q_A}{\hat{\rho}'\hat{T}'} \quad (30)$$

From the compatibility condition Eq.(25) and the definition of A_3 Eq.(20), we have

$$\tilde{\rho}' = \frac{mc}{\rho_s A \Lambda_o^{3/2}} \quad (31)$$

where ϵ is a small number defined by

$$\epsilon = \left(\frac{dq'}{dx'} \right) x' = X'$$

Substituting Eq.(31) into (30), we obtain finally for the normalized mass ablation flux

$$g' = (\gamma - 1) \left(\frac{1 + \gamma \tilde{M}^2}{1 + \frac{\gamma - 1}{2} \tilde{M}^2} \right) \frac{Q_A mc}{\rho_s \Lambda \Lambda_o^{3/2}} \frac{1}{\rho' T'}$$

Since the factor involving $\tilde{M}^2 = 2$ at most, we further approximate the above expression by

$$g' \approx (\gamma - 1) \frac{Q_A mc}{\rho_s \Lambda \Lambda_o^{3/2}} \frac{1}{\rho' T'} \quad (32)$$

The ablated mass flux, consequently, scales as

$$g \propto \frac{mq_o}{\rho_v \Lambda_o^{3/2}} \quad (32a)$$

3. Numerical analysis and results

Restricting the plasma state in the range of

$$\begin{aligned} 0.5 < T_{e0} < 5 \text{ keV}, \\ 2 \times 10^{13} < n_{e0} < 5 \times 10^{14} \text{ cm}^{-3} \end{aligned} \quad (33)$$

after guessing a value of g' , the system of equations, Eqs.(14)-(17), can be integrated numerically once proper values of ρ' , T' , E' , and q' at the pellet surface are chosen. As we anticipate the existence of an efficient shielding mechanism,

the stopping distance or the cloud boundary X should be reasonably short. In the computations, we take arbitrarily

$$X < 5 \text{ cm} \quad (34).$$

Besides, the ablatant temperature T_f at the cloud boundary X should not exceed the temperature of the ambient plasma electrons i.e.

$$T_f \leq T_{eo} \quad (35)$$

Under the restrictions of Eqs.(34) and (35) and when the ablation is a sublimation process, it was found that \hat{T}^* and $\hat{\rho}^*$ at the pellet surface must be chosen in the following range

$$\begin{aligned} 0.5 < \hat{T}^* &\leq 1 \\ 0.5 < \hat{\rho}^* &\leq 1 \end{aligned} \quad (36)$$

To ensure the existence of an effective shielding at the pellet surface, \hat{E}' must be chosen sufficiently small (e.g. < 0.05). On the other hand, to save computational time, it should not be too small (e.g. > 0.01).

The corresponding value of \hat{q}' has to be determined from the specified value of \hat{E}' consistent with the stopping power relationship of

$$\hat{q}' = \hat{E}' E_{xp} \left\{ - \int_{E_v}^{E_0} \frac{\sigma(E)}{2L(E)} dE \right\} \quad (37)$$

With all the derivatives thus determined, the integration is initiated at the pellet surface and proceeds outwards until at $x' = X'$

$$\tilde{E}' (= E/E_0) \rightarrow 1 \text{ and } \tilde{q}' (= q/q_0) \rightarrow 1 \quad (23)$$

Furthermore, we require that at $x' = X'$

$$\left(\frac{dq'}{dx'} \right)_{x'=X} < 10^{-3} \quad (24a)$$

(From Eqs.(16) and (17), it can be seen that the requirement of Eq.(24a) automatically infers that

$$\left(\frac{dE'}{dx'} \right)_{x'=X} < 10^{-3}$$

When Eq.(24a) is not satisfied, the integration has to be repeated by choosing a new value of the mass ablation flux g' . Results of numerical analysis based on such a procedure showed that the ablated mass flux scales as

$$g' \propto \frac{1}{\rho_s^{3/2}} \left(\frac{q_0}{\rho_s^2 s^3} \right) \left(\frac{m}{\rho_s} \right)^{1/2} \frac{1}{\Lambda_0} \quad (38)$$

In the range of $0.2 < E < 30$ keV, we have approximately

$$\Lambda(E) \approx 5.45 \times 10^{-3} E^{-1.65}$$

Thus, in the range of the plasma state given previously, described by Eq.(33) we have explicitly

$$\hat{g}' \hat{\rho}' \hat{T}' = 2.413 \times 10^{-29} n_{e0} T_{e0}^{3.975} \quad (39)$$

shown as the dotted line in Fig.3. For comparison, the approximate solution of Eq.(32) is indicated by the solid line.

The attenuation of the plasma electron energy and energy flux in the ablatant cloud as well as the variation of the ablatant temperature and velocity at a given

plasma state of $T_{e0} = 800\text{eV}$ and $n_{e0} = 1.0 \times 10^{14} \text{ cm}^{-3}$ are shown in Fig.1 and Fig.2 respectively.

4. Discussions

4.1. Effect of the magnetic field orientation

The treatment thus far deals only with the case where the magnetic field lines are normal to the pellet surface. In order to estimate the effect of magnetic field orientation on the ablation rate of the pellet, we shall consider the other extreme case where the field line are parallel to the pellet surface.

When plasma instabilities are absent, plasma electrons can penetrate the pellet surface only if the magnetic pressure is not too high. Assuming $T_e = T_i$, this condition can be written explicitly as

$$\frac{B^2}{8\pi} < 2 p_e \quad (40)$$

Taking a plasma state close to the upper limit of the range considered previously, Eq. (33), e.g. $n_{e0} = 2 \times 10^{14} \text{ cm}^{-3}$, and $T_{e0} = 5 \text{ keV}$, we have $B < 0.89 \text{ tesla}$ from the above expression. Comparing it with present values of the confinement field used in most tokamaks, it is rather low. Thus, when plasma instabilities are absent, the pellet ablation rate should be negligible compared with the case when the field lines are normal to the pellet surface.

4.2. Effect of expansion geometry on the pellet ablation rate

In order to examine the effect of expansion geometry on the pellet ablation rate, a comparison of the ablation rate at a given plasma state of $T_{e0} = 1 \text{ keV}$ and n_{e0}

$= 1.0 \times 10^{14} \text{ cm}^{-3}$ is made. In the case of constant area plane flow, the mass ablation rate $g = 0.78 \text{ g./cm}^2/\text{sec}$. The mass ablation flux of an idealized cylindrical pellet of infinite length and that of a spherical pellet are compared at three different radii in the following table.

Table I - Comparison of mass ablation flux g of various expansion geometry

Expansion geometry	Pellet radius r_p in mm		
	0.5	1	2
Cylindricals	1.38	0.87	0.55
Spherical	37.6	23.7	14.9

From the results shown in the above table, we observe that for a spherical pellet of reasonable size, the ablation rate is always greater than that of the plane ablated flow. The relative ablation rate for an idealized cylinder depends on its radius. For a cylinder with radius, $r_p < 1 \text{ mm}$., its ablation rate is greater than that of the plane flow at the same plasma state, while for one with radius, $r_p > 1 \text{ mm}$., the ablation rate becomes less than that of the plane flow at the same plasma state. The ablation rate of a spherical or cylindrical pellet is insensitive to the precise state of the ablatant at the pellet surface; however, it should be borne in mind that the ablation rate of the plane flow case, as shown previously by Eq. (38), is very sensitive to the ablatant state, T_v , and at the pellet surface. The above mentioned mass ablation flux, $g = 0.78 \text{ g/cm}^2/\text{s}$ is based on the assumption that the ablatant leaves the pellet surface at its surface temperature, T_s (10 K or $T' = 1$). If the ablatant temperature at the pellet surface is taken to be

comparable to the sublimation energy of 10^{-2} eV, (or $\hat{T} = 10$), the mass ablation flux according to Eq.(38) will be reduced by about an order of magnitude.

In the plasma temperature range of $0.5 < T_{eo} < 5$ keV, the mass ablation flux of the plane flow case, as shown by Eq.(39), varies with the unperturbed state of the plasma electrons as

$$g_{eo} \propto n_{eo} T_{eo}^{3.975} \quad (41)$$

In comparison, the mass ablation flux of a cylindrical or spherical pellet at a given radius, varies with the unperturbed plasma electron state of n_{eo} and T_{eo} as

$$g_{sp} \propto n_{eo}^{1/3} T_{eo}^{1.69} \quad (42)$$

The mass ablation rate in the plane flow case, is thus more sensitive to the unperturbed state of the plasma electrons.

To study the ablation of a cylindrical pellet, we have considered previously a cylinder of infinite length and consequently neglected the ablation of its ends [1]. To estimate ablation rate, of the ends we have considered the ablation of a thin disk and disregarded its side by restricting the flow to be of constant area [2]. By doing so, we have lost the inherent transonic feature of the flow of a finite cylinder. In comparison with the flow of a spherical pellet, this crude approximation indicates that the flow of a cylindrical pellet basically is two-dimensional. A clear understanding of the problem, therefore, still requires further study. On the other hand, as in most pellet injection experiments, most of the time the pellet is injected with the axis of the cylinder normal to the field lines. Following the discussion of the previous section, (the ablation rate of the ends of the cylinder is expected to be much less than that of its side), the ablation

mass flux estimated on the basis of an infinite cylinder thus could represent an upper bound of a cylinder of finite length.

Acknowledgement

F.L. Tang is grateful for the fellowship grant offered by the Commission of the European Communities.

References:

- [1] Villorosi, P. and Chang, C.T., Contributed paper in Proc. 16th European Conf. on Controlled Fusion and Plasma Physics (Venice, 1989).**
- [2] Tang, F.L. and Chang, C. T., *ibid.***
- [3] Parks, P.B.,Turnbull, R.J., *Phys. Fluids* 21 (1978) 1735.**
- [4] Chang, C.T., Rep. Risø-R-460, Risø National Laboratory, Roskilde, Denmark (1982).**
- [5]. Chang, C.T., *Phys. Fluids* 26 (1983) 805.**

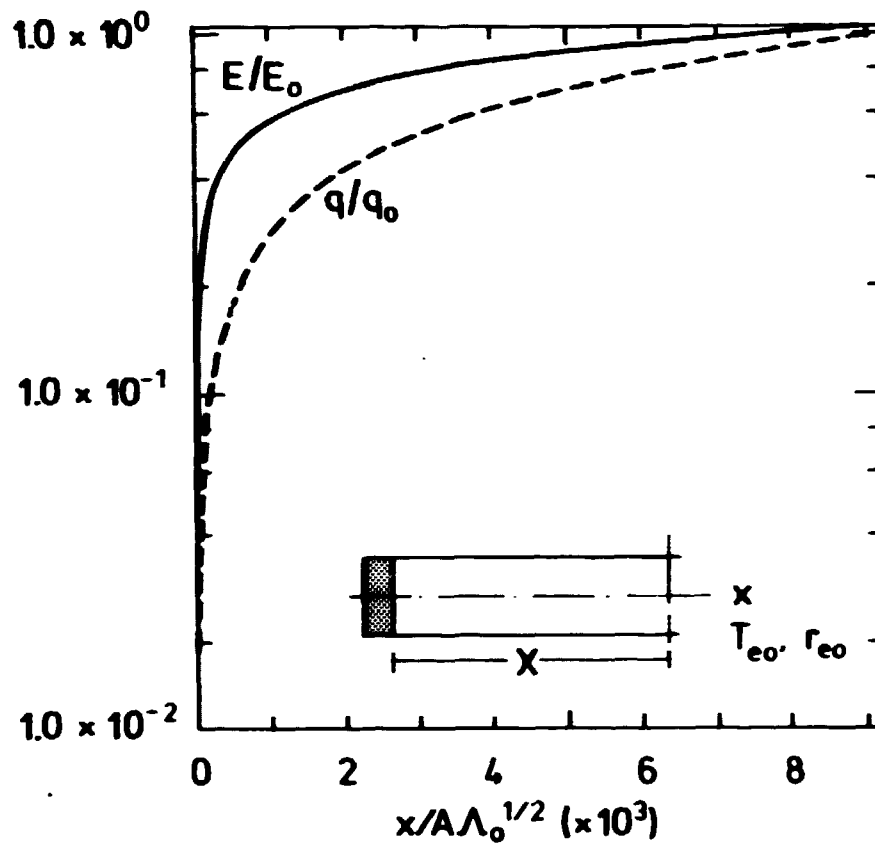


Fig.1 Attenuation of the normalized plasma electron energy, E/E_0 and energy flux q/q_0 with respect to the normalized distance from the pellet surface, $X/A\Lambda_0^{1/2}$

Plasma state: $T_{eo} = 800$ eV, $n_{eo} = 1.0 \times 10^{14}$ cm $^{-3}$. Ablatant state at the pellet surface, $T_v = T_s$ and $\rho_v = \rho_s$.

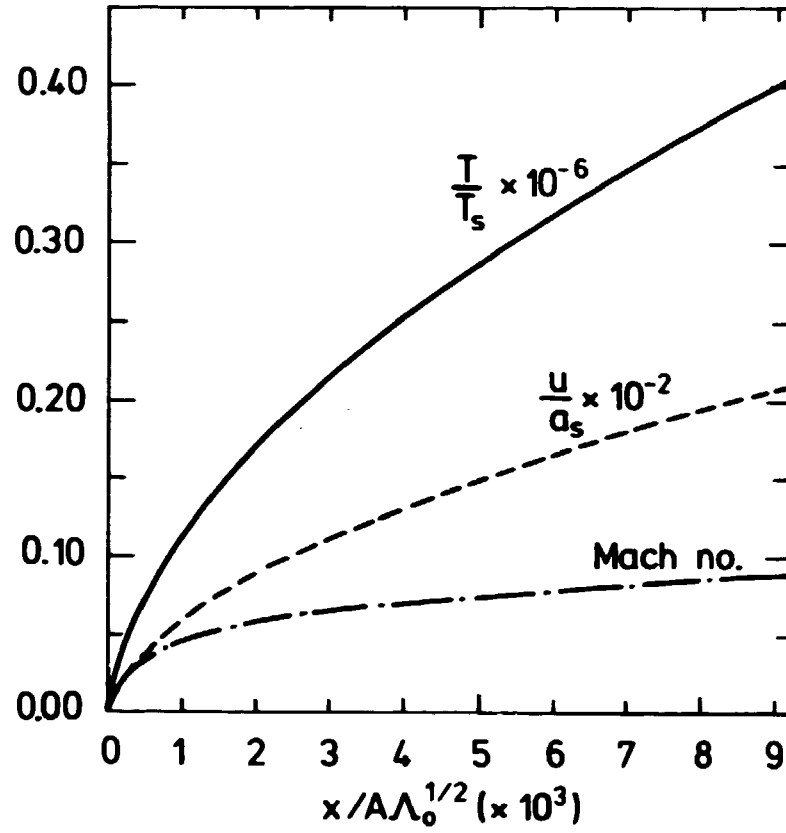


Fig.2 Variation of the normalized ablatant temperature, T/T_s ablatant flow velocity, u/a_s and the local Mach number, M with respect to the normalized distance, $X/A \Lambda_0^{1/2}$

Plasma state: $T_{e0} = 800 \text{ eV}$, $n_{e0} = 1.0 \times 10^{14} \text{ cm}^{-3}$. Ablatant state at the pellet surface, $T_v = T_s$ and $\rho_v = \rho_s$.

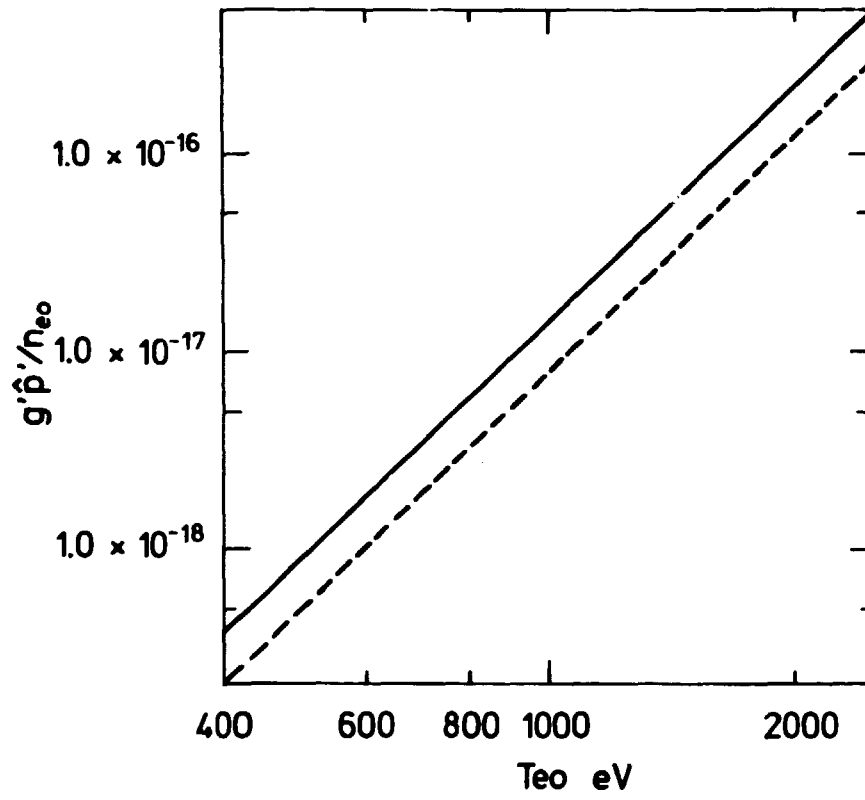


Fig.3 Variation of the normalized mass ablation flux, $g' = g/\rho_s a_s$ with respect to the ambient plasma electron temperature, T_{e0} , density, n_{e0} , and the normalized ablatant pressure, p_v/ρ_s at the pellet surface ($\hat{p}\hat{T}' = \hat{p}'$)

**Available on exchange from:
Risø Library,
Risø National Laboratory,
P.O. Box 49, DK-4000 Roskilde, Denmark
Phone 42 37 12 12, ext. 2268/2269,
Telex 43116, Telefax 46 75 56 27**

**ISBN 87-550-1508-5
ISSN 0418-6435**